Progress In Electromagnetics Research C, Vol. 51, 11–18, 2014

A Dual-Broadband Circularly Polarized Antenna with Unidirectional Radiation Pattern

Neng-Wu Liu*, Ya-Li Yao, Zhi-Ya Zhang, Yang Li, Guang Fu, and Shao-Li Zuo

Abstract—A dual-band circularly polarized (CP) antenna with wide axial ratio (AR) and impedance bandwidths is proposed. Based on a rectangular ground, the antenna consists of a trapezoid patch, an L-shaped strip, a cavity, and T-shaped and L-shaped perturbations. By embedding a feeding line with a trapezoid patch and an L-shaped strip, dual-band input impedance performance and a CP performance at upper band are obtained. In order to achieve a CP performance at the lower band, a T-shaped perturbation is embedded inside the slot. Moreover, the CP performance is enhanced by inserting an L-shaped perturbation at the right bottom corner of the slot. Furthermore, using a cavity underneath the antenna, unidirectional radiation patterns with greatly gain enhancement are obtained. The measured results show that the impedance bandwidths for $S_{11} < -10$ dB are 22.7% (2.34–2.94 GHz) and 79.8% (4.64–10.8 GHz) while the axial ratio bandwidths (AR < 3 dB) are 26.4% (2.3–3 GHz) and 12.6% (5.2–5.9 GHz) at the lower and upper bands, respectively. Additionally, the measured gain is more than 7.4 dB and 2.4 dB in the two operating bands, respectively. Thus, the antenna can be well applied for both 2.4/5.8 GHz WLAN bands and 2.5/5.5 GHz WiMAX bands.

1. INTRODUCTION

Recently, dual frequency bands at 2.4 and 5.5 GHz [1–3] are popularly used in wireless local area network (WLAN: 2.4–2.48 and 5.72–5.85 GHz) and the worldwide inter operability for microwave access (WiMAX: 2.5–2.69 and 5.25–5.85 GHz), and antennas with good performances appear to be a key factor to assure communication quality. For the application, the demand for antennas with circularly polarized (CP) performance is becoming trendy due to the reduction in multipath effects and the flexibility in the orientation angle between transmitter and receiver [4, 5].

In WLAN/WiMAX applications, the performances of a CP antenna are justified by both axial ratio (AR) and impedance bandwidths, where the AR bandwidth needs to be larger than 10%. In order to meet these requirements, multi-feed configurations have been proposed in several antennas recently, including a 90° hybrid feed network [6], a switch line balun [7] and a Γ-shaped feed [8]. However, these structures are complicated, and single-feed configurations are preferred. Thus several single-feed CP antennas have been proposed in [9–18]. In [9], a coplanar-strip dipole antenna achieves a 3-dB AR bandwidth of 50%. Using a coplanar capacitive feed and a slot, the antenna [10] has an 3-dB AR bandwidth of 7.1%. A single coaxial probe in [11] used to excite circularly polarized patterns achieves an 3-dB AR bandwidth below 7%. Although these antennas have many advantages, only single band is obtained in the designs, which cannot cover the whole WLAN/WiMAX bands. In order to obtain dual-band CP performance, several antennas are also proposed by utilizing T-strip with fork-shaped monopole [12, 13], combining a Y-shaped radiating patch [14], using a U-strip slot [15] and inserting a shorting metallic cylinder [16]. Unfortunately, all of them have narrow AR bandwidth less than 10% in the two operating bands. It is also noted that antennas for some applications in the dual bands, such

Received 13 April 2014, Accepted 1 June 2014, Scheduled 12 June 2014

* Corresponding author: Neng-Wu Liu (nengwuliu@126.com).

The authors are with the Science and Technology on Antenna and Microwave Laboratory, Xidian University, Xi'an 710071, People's Republic of China.

as Wi-Fi access points [17], gap fillers [18], and RFID readers [19], require a unidirectional pattern to provide high security and efficiency of the propagation channels. Therefore, it is desired to design a dual-band and reflector-backed antenna for CP operation.

In this paper, a coplanar waveguide (CPW) antenna with dual-band circularly polarized characteristic is proposed. The antenna is based on a rectangular ground. Using a CPW feeding line with a trapezoid patch and L-shaped strip, the antenna achieves dual-band input impedance performance and a CP performance at upper band. By introducing T-shaped and L-shaped perturbations inside the slot, dual-band CP performance covering the WLAN/WiMAX can be achieved. Moreover, the antenna can obtain unidirectional radiation patterns and greatly improve gain by placing the cavity underneath the antenna.

2. ANTENNA DESIGN AND DISCUSSIONS

Figure 1 shows the configuration of the proposed antenna, which is fabricated on an FR4 epoxy substrate with a relative permittivity of 4.4, thickness of 2 mm and loss tangent of 0.02. Composed of a trapezoid patch, an L-shaped strip, a cavity, T-shaped and L-shaped perturbations, the proposed antenna is fed

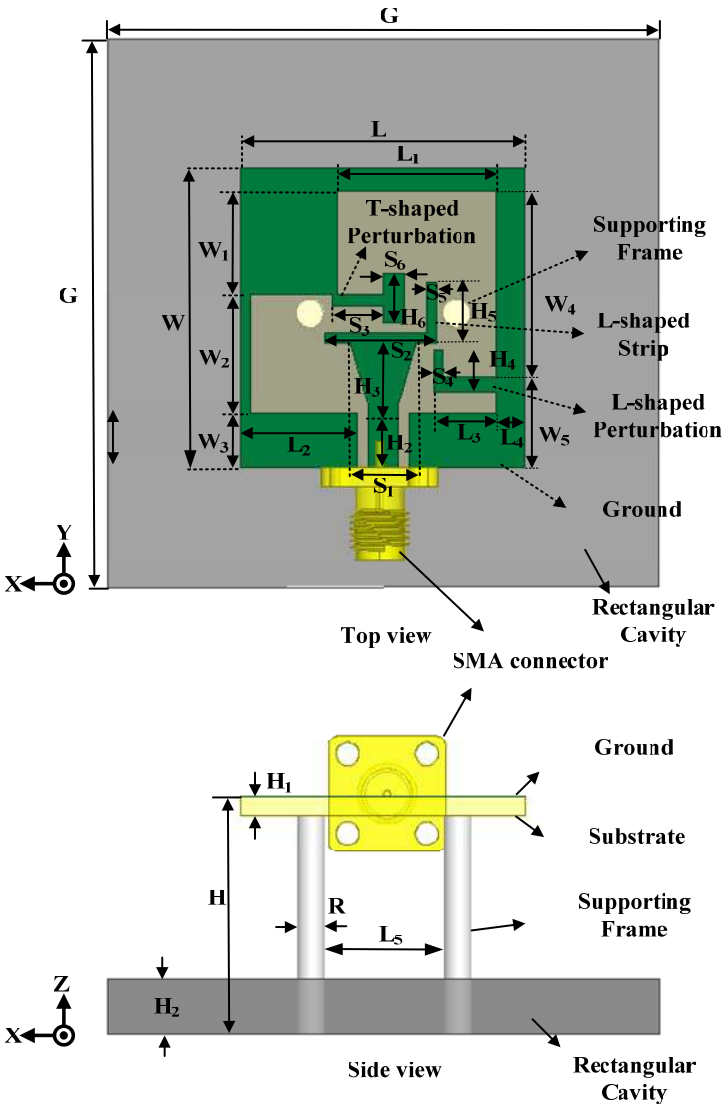

Figure 1. Geometry of the antenna.

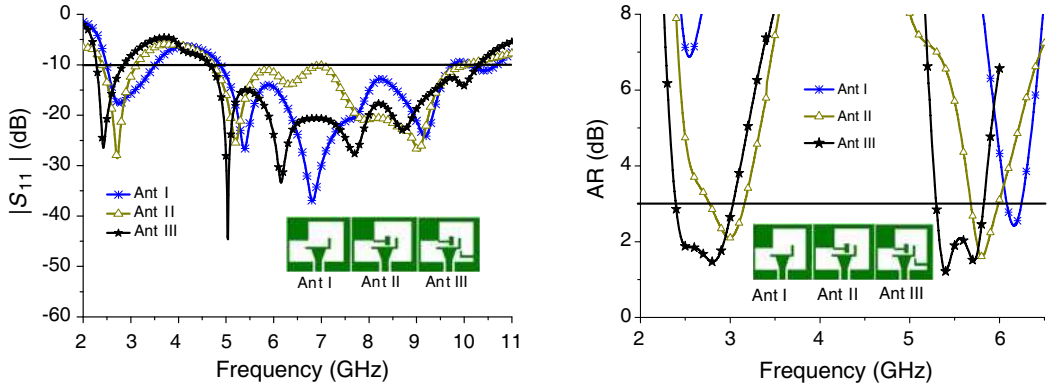

(a) (b)

Figure 2. Simulated results for Ants. I -III: (a) S_{11} and (b) AR.

Table 1. Dimensions of the proposed antenna.

Parameters	L	L_1	L_2	L_3	L_4	L_5	W	W_1	W_2
Values/mm	31	17.3	11.6	6.8	3.2	13	33	11.4	13
Parameters	W_3	W_4	W_5	H	H_1	H_2	H_3	H_4	H_5
Values/mm	6	20.3	10.1	26	2	7	6.8	4.3	6.7
Parameters	H_6	S_1	S_2	S_3	S_4	S_5	S_6	R	G
Values/mm	5.5	7.28	12.3	5.5	1	1.4	2.3	3	60

by a CPW feeding line, where the signal strip and gaps have widths of 3.2 and 1.2 mm, respectively. The trapezoid patch is employed to connect with the end of the CPW feeding line to ensure the well-matched impedance in the operating band, and its the design procedure is illustrated in Figure 2. The optimal parameters for the antenna are listed in Table 1.

More specifically, as depicted in Ant I, which consists of an L-shaped strip, a trapezoid patchand a ground, the structure provides good impedance matching in both of the bands, but it has a single 3-dB axial ratio operating band. Since E_θ and E_Φ components are produced by vertical and horizontal parts of the L-shaped strip, respectively, and the current phase on the vertical component is 90° delayed with respect to that of the horizontal one, the antenna (Ant I) can generate a left-hand CP (LHCP) pattern. To achieve CP performance at the lower band, a T-shaped perturbation is added to the left top corner of Ant I. As a result, dual-band CP performance at about 3 and 5.8 GHz is achieved in Ant II. Through the coupling between T-shaped perturbation and L-shaped strip above the trapezoid patch, Ant II eventually generates the right-hand CP radiation at the lower band. To further enhance the AR bandwidth, an additionally L-shaped perturbation is embedded at the right bottom corner of the slot as shown in Ant III. It can lengthen the vertical and horizontal parts of the current. Finally, the antenna achieves a 3-dB axial-ratio and impedance bandwidths of 23.2% (2.4–3.03 GHz), 21.4% (2.29–2.84 GHz) for the lower band and 9.4% (5.3–5.82 GHz), 75.3% (4.67–10.31 GHz) for the upper band, respectively. The surface current distributions of the proposed antenna at 2.5 and 5.8 GHz are presented in Figure 3. It can be seen that the horizontal and vertical surface currents can be combined and equivalent to a tilted current. The tilted currents at the four phases (0°, 90°, 180°, and 270°) are mutually orthogonal, so that the antenna can excite the RHCP and LHCP at the lower and upper bands, respectively. All parameters of the proposed antenna are optimized using the Ansoft HFSS 14.

To investigate the influence of the related geometrical dimensions on the proposed antenna performance, a discussion on the key parameters of the antenna is presented. Throughout the study presented in this section, only one parameter is changed at one time with all other parameters fixed to the values listed in Table 1. Based on the analysis above in Figures 2 and 3, the L-shaped perturbation plays a key role in AR performance. Thus, the effect of different lengths of the L-shaped perturbation

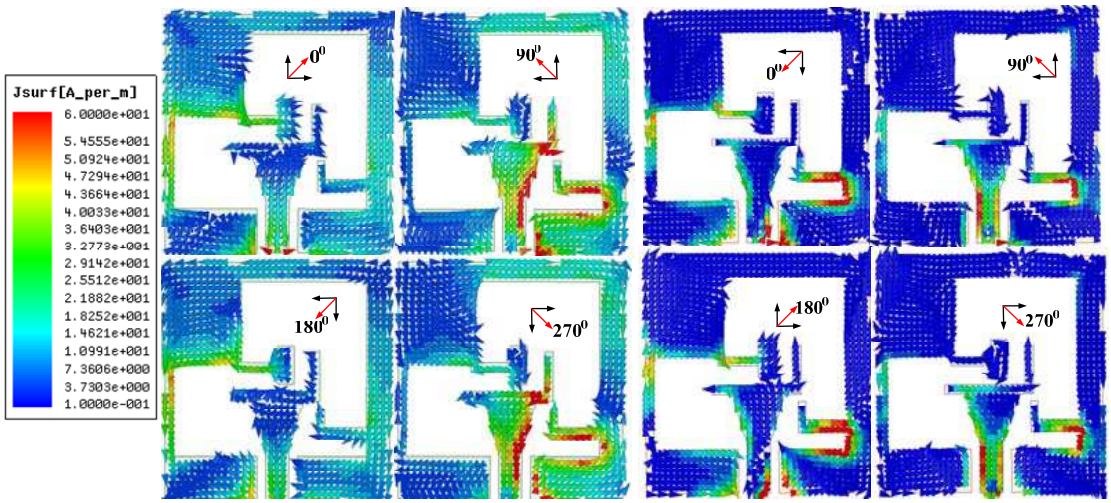

Figure 3. Surface current density distributions of the antenna: (a) 2.5 and (b) 5.8 GHz.

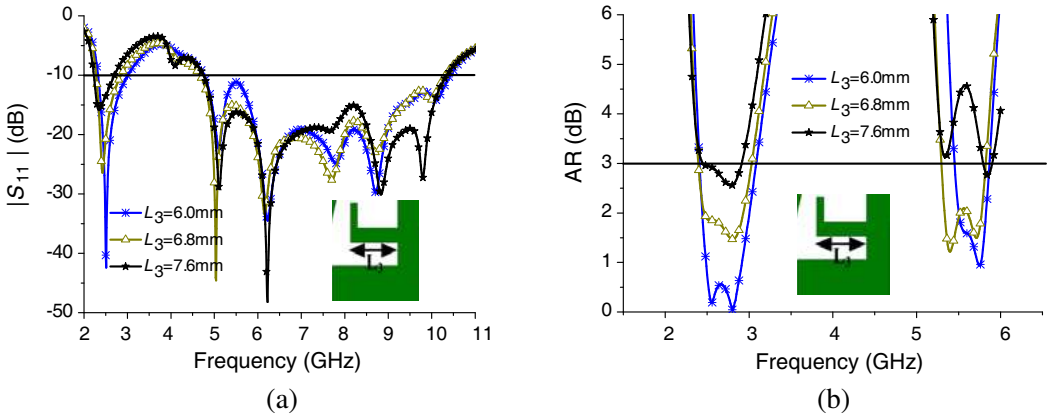

Figure 4. Effects of various L_3 on the antenna performance: (a) S_{11} and (b) AR.

(L_3) is analyzed. Figure 4 shows the simulated reflection coefficient and axial ratio with variation of L_3. As shown in Figure 4(a), an increase about L_3 results in a decrease in the center frequency of the lower band with the upper impedance bandwidth unchanged. From Figure 4(b), the 3-dB AR at the upper band shifts to the lower frequency as L_3 increases, which shows that the upper resonant frequency is determined by the L-shaped perturbation at the right bottom corner of the slot. Finally, L_3 is chosen as 6.8 mm to ensure better impendence and 3-dB AR bandwidths.

Additionally, the effect of different lengths of the L-shaped strip (H_5) on reflection coefficient and AR is analyzed. The increase in H_5 has little influence on the reflection coefficient as shown in Figure 5(a). The 3-dB AR bandwidth at the upper band in Figure 5(b) moves to the lower frequency with the increase in H_5, whereas the AR at the lower band changes slightly. All these results indicate that the L-shaped strip above the trapezoid patch mainly affects the AR bandwidth of the upper band. Hence, an overall good AR bandwidth has been obtained when $H_5 = 6.7$ mm.

Moreover, through the coupling between T-shaped perturbation and L-shaped strip above the trapezoid patch, a lower CP mode can be preliminary generated by splitting the fundamental resonant mode into two near-degenerate modes along the orthogonal edges of the initial ground. Thus the T-shaped perturbation becomes a key factor in the CP radiation. Figure 6 illustrates the influence of the width (W_1) on the antenna performance. Note that an increase in W_1 decreases the distance between the T-shaped perturbation and L-shaped strip, so the coupling between them is enhanced. It

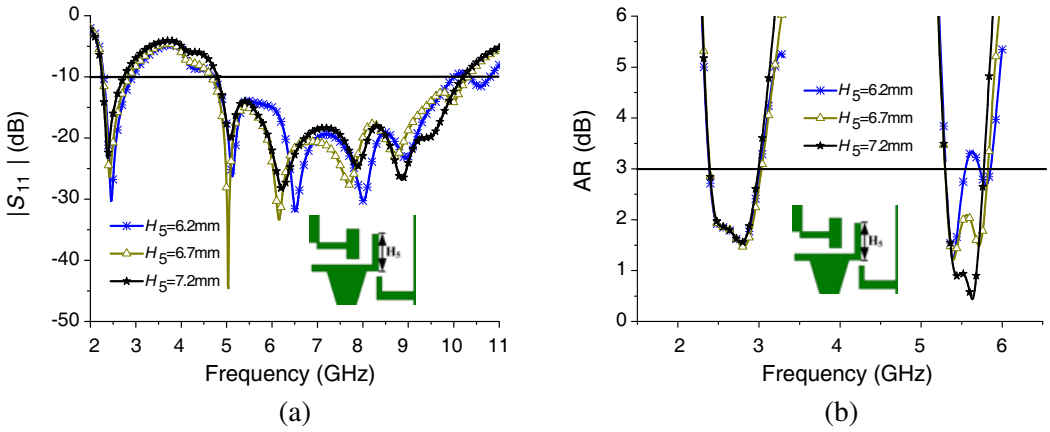

Figure 5. Effects of various H_5 on the antenna performance: (a) S_{11} and (b) AR.

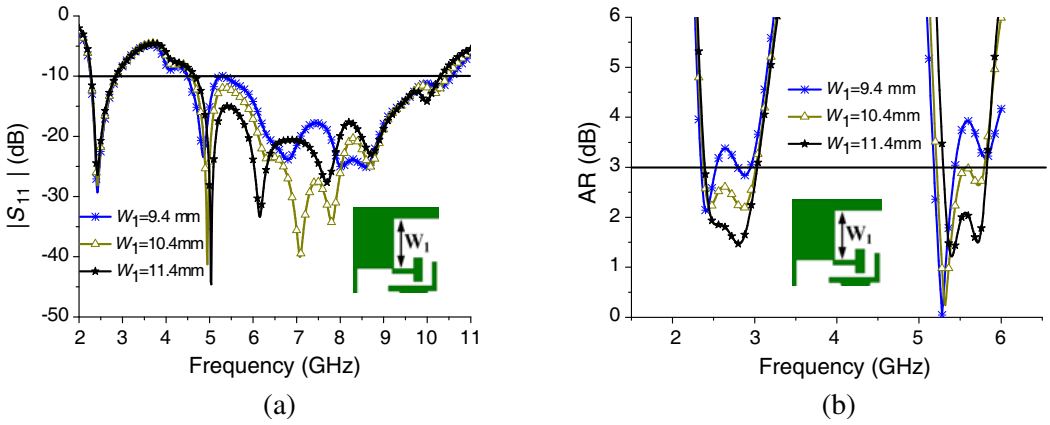

Figure 6. Effects of various W_1 on the antenna performance: (a) S_{11} and (b) AR.

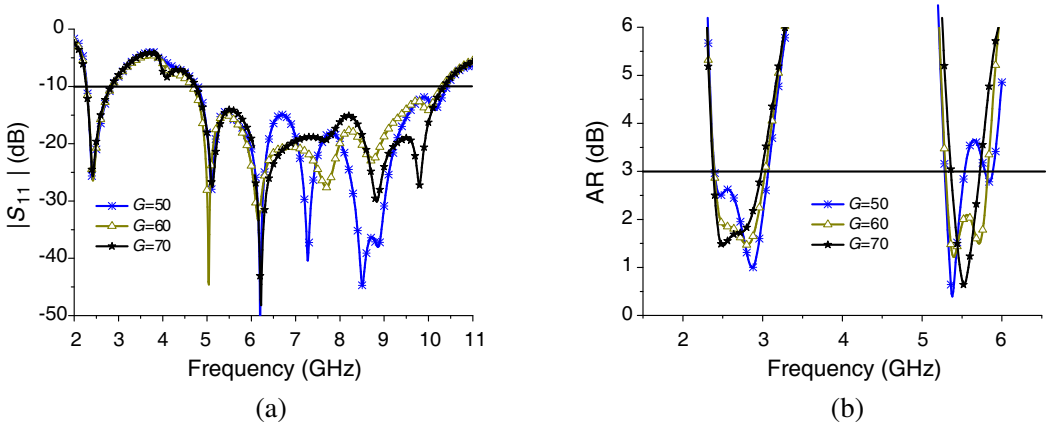

Figure 7. Effects of various G on the antenna performance: (a) S_{11} and (b) AR.

greatly enhances AR performance. Thus, the width (W_1) is of great significance for creating the AR bandwidth. Furthermore, since the reflector can disturb and redistribute the surface current on the antenna, the return loss and AR results can be affected by the dimension of the reflector. As shown in Figure 7, the AR bandwidth is influenced by the dimension of the reflector. By selecting $W_1 = 11.4\,\text{mm}$ and $G = 60\,\text{mm}$, better impendence and 3-dB AR bandwidths which can meet the requirement for WLAN/WiMAX standards are achieved.

3. RESULTS AND DISCUSSION

A prototype of the CPW antenna is fabricated as shown in Figure 8. The measurements were carried out using Agilent E8363B vector network analyzer and anechoic chamber. In Figure 9, it can be seen that the measured impedance bandwidths for $S_{11} < -10$ dB are 2.34–2.94 GHz and 4.64–10.8 GHz. The simulated and measured AR values against frequency are depicted in Figure 9(b), and the measured result for AR < 3 dB is approximately from 2.3–3 GHz and 5.2–5.9 GHz, successfully covering 2.4/5.8 GHz WLAN and 2.5/5.5 GHz WiMAX bands. The discrepancy between the measured and simulated results is caused by the introduction of the fabrication tolerance.

The normalized radiation patterns of the proposed antenna at 2.5, 5.5 and 5.8 GHz in XZ-plane and YZ-plane are shown in Figure 10. It can be observed that unidirectional radiation patterns are obtained due to the cavity. For the lower band (2.3–3 GHz), excellent RHCP radiation patterns can be observed. The LHCP radiation patterns in the upper band (5.2–5.9 GHz) are a little tilted, which is mainly caused by the asymmetrical structure of the proposed antenna. Additionally, the cross-polarizations can keep 16 dB lower than the co-polarizations in $+Z$ direction ($\theta = 0°$, $\Phi = 0°$). Thus the antenna is well applied to both WLAN/WiMAX bands.

Figure 11 shows the measured gain of the proposed antenna in broadside direction. The measured peak gain is over 7.4 dB from 2.4 to 3 GHz. Within the upper band, the measured gain is above 2.4 dB, which is much higher than that of the common dual-band CP antennas. Note that, due to the asymmetric radiation pattern, the measured gains in the upper band are not as good as the practical peak gains of the antenna, which may need to be improved in the future.

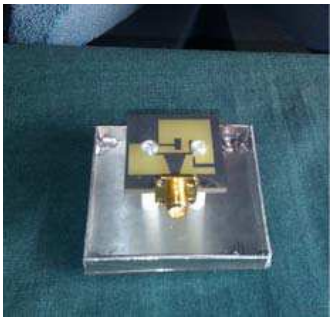

Figure 8. Photograph of the fabricated antenna.

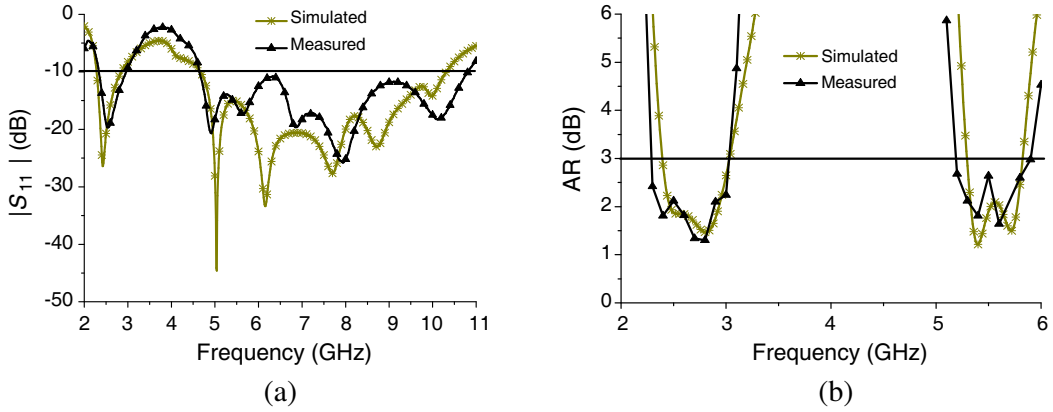

Figure 9. Simulated measured results of the proposed antenna: (a) S_{11} and (b) AR.

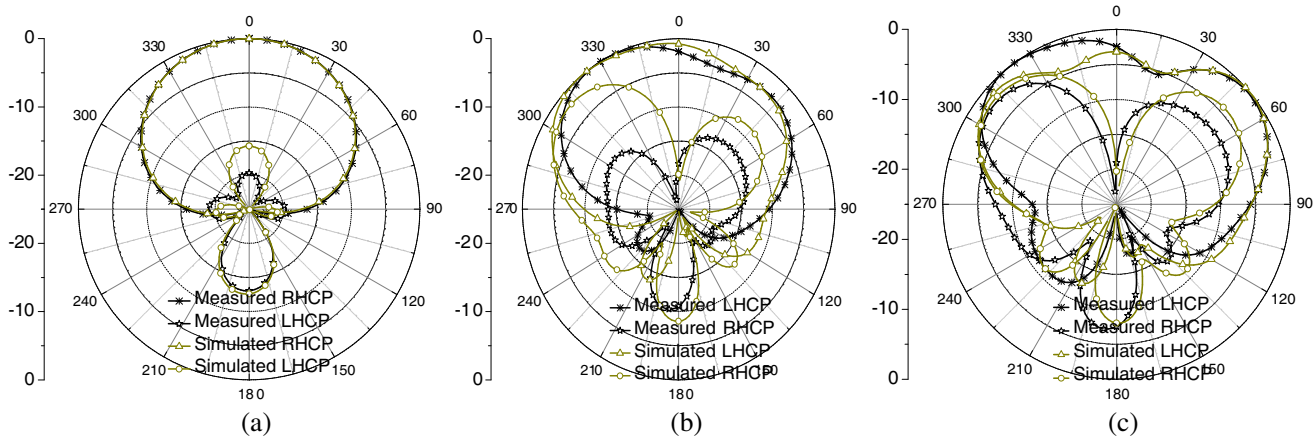

Figure 10. Normalized radiation patterns of the proposed antenna at (a) 2.4, (b) 5.5, and (c) 5.8 GHz.

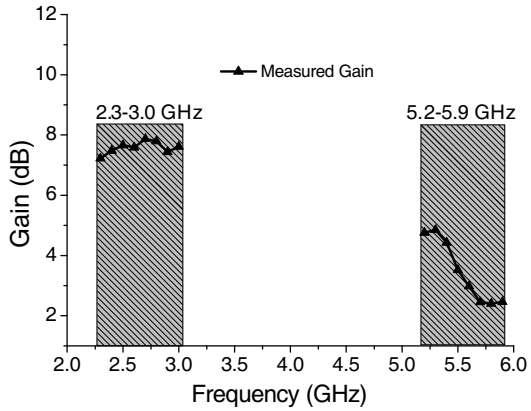

Figure 11. Measured gain for the proposed antenna.

4. CONCLUSION

A unidirectional dual-band CP antenna is proposed. Using a CPW feeding line with a trapezoid patch and L-shaped strip, the antenna achieves dual-band input impedance performance and a CP performance at upper band. By introducing T-shaped and L-shaped perturbations inside the slot, dual-band CP performance covering the WLAN/WiMAX can be achieved. Finally, the antenna achieves a 3-dB AR and impedance bandwidths of 26.4%, 22.7% for the lower band and 12.6%, 79.8% for the upper band, respectively. A cavity is utilized to achieve high gain and decreases undesirable back radiation. Good agreement is achieved between the measured and simulated results, indicating that the proposed antenna can be a good candidate for WLAN/WiMAX applications.

ACKNOWLEDGMENT

The authors would like to thank Professor Guang Fu for valuable suggestions. This work was supported by the Fundamental Research Funds for the Central Universities (Nos. K5051302033 and K5051307009).

REFERENCES

1. Zhang, Z. Y., G. Fu, and S. L. Zuo, "A compact printed monopole antenna for WLAN and WiMAX applications," *Microwave Opt. Technol. Lett.*, Vol. 52, No. 4, 857–861, Apr. 2010.

2. Wang, H. and M. Zheng, "An internal triple-band WLAN antenna," *IEEE Antenna and Wireless Propag. Lett.*, Vol. 10, 569–572, Jun. 2011.
3. Lin, D. B., I. T. Tang, and Y. J. Wei, "Compact dual-band-notched CPW-fed wide-slot antenna for WLAN and WiMAX applications," *Microwave Opt. Technol. Lett.*, Vol. 53, No. 7, 1496–1501, Apr. 2011.
4. Hsu, S.-H. and K. Chang, "A novel reconfigurable microstrip antenna with switchable circular polarization," *IEEE Antenna and Wireless Propag. Lett.*, Vol. 6, 160–162, Feb. 2007.
5. Sung, Y. J., T. U. Jang, and Y.-S. Kim, "A reconfigurable microstrip antenna for switchable polarization," *IEEE Microw. Wirel. Compon. Lett.*, Vol. 14, No. 11, 534–536, Nov. 2004.
6. Zhang, Z. Y., N. W. Liu, J. Y. Zhao, and G. Fu, "Wideband circularly polarized antenna with gain improvement," *IEEE. Antenna Wireless Propagt. Lett.*, Vol. 12, 456–459, 2013.
7. Wu, Z. H., Y. Lou, and E. K. Yung, "A circular patch fed by a switch line balun with printed L-probes for broadband CP performance," *IEEE. Antenna Wireless Propagt. Lett.*, Vol. 6, 608–611, 2007.
8. Fu, G., Z. Y. Zhang, S. L. Zuo, J. Lei, and S. X. Gong, "A wideband circularly polarized antenna with Γ-shaped feed," *Microw. Opt. Technol. Lett.*, Vol. 54, No. 1, 153–156, Jan. 2012.
9. Tsai, C.-L., "A coplanar-strip dipole antenna for broadband circular polarization operation," *Progress In Electromagnetics Research*, Vol. 121, 141–157, 2011.
10. Kasabegoudar, V. G. and K. J. Vinoy, "A broadband suspended microstrip antenna for circular polarization," *Progress In Electromagnetics Research*, Vol. 90, 353–368, 2009.
11. Zainud-Deen, S. H., H. A. Malhat, and K. H. Awadalla, "A single-feed cylindrical super quadric dielectric resonator antenna for circular polarization," *Progress In Electromagnetics Research*, Vol. 85, 409–424, 2008.
12. Chen, C. H. and E. K. N. Yung, "Dual-band circularly-polarized CPW-fed slot antenna with a small frequency ratio and wide bandwidths," *IEEE Trans. Antennas Propag.*, Vol. 59, No. 4, 1379–1384, Apr. 2011.
13. Chen, C. H. and E. K. N. Yung, "Dual-band dual-sense circularly-polarized CPW-fed slot antenna with two spiral slots loaded," *IEEE Trans. Antennas Propag.*, Vol. 57, No. 6, 1829–1833, Jun. 2009.
14. Wu, T., X. W. Shi, P. Li, and H. Bai, "Trip-band microstrip-fed monopole antenna with dual-polarization characteristics for WLAN and WiMAX applications," *Electron. Lett.*, Vol. 49, No. 25, Dec. 2013.
15. Li, W. M., B. Liu, and H. W. Zhao, "The U-shaped structure in dual-band circularly polarized slot antenna design," *IEEE Antenna and Wireless Propag. Lett.*, Vol. 13, 447–450, Mar. 2014.
16. Deng, C. J., Y. Li, Z. J. Zhang, G. P. Pan, and Z. H. Feng, "Dual-band circularly polarized rotated patch antenna with a parasitic circular patch loading," *IEEE Antenna and Wireless Propag. Lett.*, Vol. 12, 447–450, Apr. 2013.
17. Medeiros, C. R., E. B. Lima, J. R. Costa, and C. A. Fernandes, "Wideband slot antenna for WLAN access points," *IEEE Antenna and Wireless Propag. Lett.*, Vol. 9, 79–82, 2010.
18. Kim, B., J. Ryu, H. Choo, H. Lee, and I. Park, "Dual ISM-band gap-filler microstrip antenna with two Y-shaped sots for satellite internet service," *Microwave Opt. Technol. Lett.*, Vol. 52, No. 8, 1825–1827, Aug. 2010.
19. Mobashsher, A. T., M. T. Islam, and N. Misran, "A novel high-gain dual-band antenna for RFID reader applications," *IEEE Antenna and Wireless Propag. Lett.*, Vol. 9, 653–656, Apr. 2010.